Growth Rate of Extended-Chain Crystals: The Lateral Surface Free Energy of Pure n-$C_{94}H_{190}$ and a Fraction $\sim C_{207}H_{416}$

John D. Hoffman

Engineering Materials Program, Department of Chemical and Nuclear Engineering, University of Maryland, College Park, Maryland 20742. *Received June 22, 1984*

ABSTRACT: A treatment based on surface nucleation theory is given for the growth rate of extended-chain crystals. Pure materials and polydisperse fractions are considered. The growth rate near the melting point T_m is predicted to be of the form $G = K(T_0 - T_x)$ where T_x is the crystallization temperature, and T_0 a temperature near T_m for a pure material and well below T_m for a fraction. The quantity $T_m - T_0$ depends on the effective value of the end (i.e., methyl group) surface free energy σ', and K is related to the lateral surface free energy σ. Previously unpublished measurements on the growth rate from the melt of high-purity n-$C_{94}H_{190}$ (C-94) are analyzed and found to conform to the predicted growth rate law. From K it is found that σ is 13.8 ± 2.1 erg cm^{-2}. The same form of growth law is predicted for crystallization of polydisperse extended-chain systems from dilute solution. An example is found in published data for a polyethylene fraction corresponding to ~C-207 crystallizing in the extended-chain mode from solution; here σ is roughly 11 erg cm^{-2}. Thus, the σ of 11–14 erg cm^{-2} that appears in the product $\sigma\sigma_e$ in the theory of polyethylene crystallization with chain folding is independently verified by a new method. As predicted, σ' is larger than σ for a fraction, where the end surface is rough; σ' may be smaller than σ for a pure compound. One overall conclusion is that in the n-hydrocarbon system, essentially the same value of σ operates in extended-chain crystallization, chain-folded crystallization in polyethylene, and in homogeneous nucleation in the n-paraffins ~C-15 and longer. The differences between the kinetics of extended-chain and chain-folded crystallization are highlighted, and the transition between the two types is discussed. Some challenges that remain regarding surface nucleation theory as it is applied to crystal growth in chain systems are noted.

I. Introduction

The principal objectives of this paper are (a) to elucidate from a theoretical point of view the factors in the n-hydrocarbon system that control the rate of extended-chain crystallization, as contrasted with the chain-folded type, (b) experimentally to test the predicted growth rate laws for extended chains, especially with regard to the growth rate as a function of undercooling and the magnitude of the lateral surface free energy σ as a function of chain length, and (c) to authenticate the σ found in earlier growth studies on chain-folded polyethylene fractions by comparing it with that found in the present work on extended chains, as well as that deduced from published homogeneous nucleation studies on n-alkanes. Although the emphasis is on extended-chain materials, the work serves also as a rather broad test of nucleation theory in various applications in the n-hydrocarbon system.

In growth rate studies on polyethylene crystallizing in the lamellar chain-folded mode, the lateral surface free energy σ plays a significant role.[1] Near the melting point, the spherulite or axialite growth rate is largely determined by the factor $\exp[-K_g/T(\Delta T)]$, where K_g, which can be determined experimentally, contains $\sigma\sigma_e$ in which σ_e is the fold surface free energy. In the above, T is the crystallization temperature, and ΔT the undercooling. The experimental value of $\sigma\sigma_e$ is close[2] to 1060 erg^2 cm^{-4} for polyethylene if $T_m°$, the equilibrium melting point for a high molecular weight fraction, is set at 418.7 K = 145.5 °C. There are a number of independent ways to measure the fold surface free energy σ_e for polymer lamellae. One of them, namely, the T_m' vs. $1/l$ plot, is essentially thermodynamic in character[1] and leads to a value for σ_e for chain-folded polyethylene lamellae that is usually accepted to be close to 90 erg cm^{-2}. From this we find for polyethylene crystallizing in the chain-folded manner that $\sigma \cong 1060/90$ or about 12 erg cm^{-2}. Values of σ ranging from about 11 to 14 erg cm^{-2} have been reported by this method.[1,2] (Most of the variation in the σ just cited relates to the fact that K_g, and hence $\sigma\sigma_e$, depends on the $T_m°$ chosen for the analysis. There are conflicting opinions[3,4] on the exact value that should be chosen for $T_m°$ for polyethylene but this has little effect on σ.[5]) It is obvious that it would be highly desirable to find some independent way to verify the σ of about 11–14 erg cm^{-2} found strictly from studies on chain-folded polyethylene. Otherwise σ as determined in the manner described above for this polymer might be regarded simply as an ad hoc parameter in the kinetic theory of polymer crystallization with chain folding.

The present work deals in one aspect with an effort to obtain an independent estimate of σ from previously unpublished crystallization rate data on highly purified n-tetranonacontane, n-$C_{94}H_{190}$, which hereafter we denote C-94. Some details of the growth rate measurements on extended-chain C-94 are given, inasmuch as unusual accuracy (±0.001 °C) in temperature control was required. Unlike the case of the crystallization kinetics of polyethylene, which gives the product $\sigma\sigma_e$, the growth kinetics of C-94 crystallized from the melt leads rather more directly to a value of σ. The theory used in the analysis of the growth rate data is based on the concept of growth controlled by surface nucleation and is carried out for both regime I and regime II. A value of σ also is obtained from published growth studies on a polyethylene fraction corresponding to $C \cong 207$ which had an M_w/M_n of 1.07 that was crystallized from dilute solution in the extended-chain form. The value of σ for C-207 is similar to that found for C-94, but is less accurate because of the uncertainties in the correction for the effect of polydispersity. The regime in each of the above cases was determined by an appropriate adaption of the Lauritzen Z test to extended-chain crystallization.

Our previously apparent concern[1] about the value of σ was heightened in part by some comments by Point and Kovacs,[6] who suggested that σ, for extended-chain poly(ethylene oxide) fractions at least, was far too small to be credible, and apparently acted as if it were strongly dependent on the length of the chain. This led them to state that the current theories of polymer crystal growth were seriously flawed because of the failure of some basic postulate. We do not find such behavior for the polyethylene fraction C-207 and pure C-94 crystallizing in the extended-chain mode. In fact, we reach the conclusion that close to the same value of σ operates in stem addition energetics

0024-9297/85/2218-0772$01.50/0

in chain-folded polyethylene lamellae, in a pure *n*-paraffin and a polyethylene fraction crystallizing in the extended-chain mode, and in homogeneous nucleation in the *n*-alkanes. Thus, we shall show that coherent surface nucleation theory emerges at least seemingly intact in this instance.

There is another reason for our present efforts on the growth kinetics of extended-chain crystals. Considerable interest attaches to the question of what happens in detail when chains become long enough to show once- and twice-folding and so on. Progress toward answering the question of the onset of chain folding with increasing chain length and undercooling depends partly on having new information concerning extended-chain crystallization. Here we have attempted to take steps in this direction. Some of the insights derived therefrom are discussed at the end of the paper.

The crystallization of chain compounds in the extended-chain mode is of basic interest in its own right and exhibits some special features. For example, our work suggests the presence of a critical undercooling $\Delta T_0 = T_m - T_0$ that must be exceeded before growth can begin at all. The fact that T_0 is below T_m (or the dissolution temperature $T_d°$ in the case of solution-grown crystals) derives in essence from the way the effective value of the end (i.e., methyl group type) surface free energy σ' operates at sufficiently low undercoolings in preventing substrate completion in isolated monolayer crystals with rough end surfaces. The difference between $T_d°$ and T_0 is very large in the extended-chain fraction C-207, as we shall show by an analysis of the data of Leung and Manley.[7]

Certain challenges that still confront nucleation theory are noted in the Discussion.

II. Theory

Thermodynamic Preliminaries. Consider a large multilayered extended-chain crystal of an ideal pure compound. Let there be n_l layers, each with a thickness l_x that corresponds to the length of a chain molecule, so that the overall dimension of the crystal collinear with the chain axes is $l = n_l l_x$. The length of each chain is given by $l_x = l_u x$ where l_u is the length of a chain unit and x the number of chain units. Also let the other two dimensions at right angles to the chain axes each be denoted y. Then let the surface free energy associated with the two chain-end type surfaces exposed to the melt be denoted σ', and the lateral surface free energy associated with the other four surfaces be σ. From this we have

$$\Delta\phi_{crystal} = 2y^2\sigma' + 4yn_l l_x\sigma - n_l l_x y^2(\Delta f)$$
$$= 2y^2\sigma' + 4yl\sigma - ly^2(\Delta f) \quad (1)$$

where Δf is the driving force for crystallization. This is

$$\Delta f = \Delta h_f(T_m - T)/T_m \quad (2)$$

where Δh_f is the heat of fusion (usually in erg cm^{-3}), $T_m = T_m(l_x)$ the melting point of a large multilayered crystal consisting of stacks of lamellae each consisting of molecules of length l_x, and T the crystallization temperature. The value of Δh_f refers to the heat of fusion relevant to l_x. The melting point of the crystal where $l_x \to \infty$ is denoted $T_m°$. The free energy of fusion corresponding to eq 2 on a per molecule basis is

$$\Delta F_c = a_0 b_0 l_x \Delta h_f((T_m - T)/T_m) \quad (3)$$

where $a_0 b_0$ is the cross-sectional area of the chain. It can be shown that eq 2 and 3 are consistent with specifiable limits for the chain lengths of interest here with the treatment of Flory and Vrij,[8] where enthalpic and entropic effects associated with localization of the chain ends are the principal cause of the melting point of a crystal with finite l_x falling from $T_m°$ to $T_m = T_m(l_x)$. Equations 1 and 2 are the defining relations for σ and σ'.

It is readily determined by setting $\Delta\phi_{crystal}$ equal to zero, which establishes the condition of equilibrium between crystal and melt, that $T = T_m = T_m°$ for a very large crystal where $l_x \to \infty$. It is of more interest to carry out the same procedure for the case $n_l = 1$, i.e., the case of an *isolated* extended-chain lamella with molecules of length l_x whose σ' surface is in contact with the melt. The result for a lamella with large y is

$$T_0 = T_m\{1 - 2\sigma'/\Delta h_f l_x\} \quad (4)$$

Thus, the melting point T_0 of an isolated lamella is lower than $T_m = T_m(l_x)$ by an amount that is governed among other factors by the end (i.e. methyl group) surface free energy σ'. This is important, since it means, as will be seen shortly, that growth processes cannot begin on the lateral surface of an isolated lamella until the crystallization temperature is below T_0. Because chain-end localization effects are accounted for in causing $T_m°$ to fall to T_m for the multilayered crystal, σ' may be only a quite small quantity comparable to or even considerably less than σ in a pure material with minimal roughness on the σ'-type surface.

Three extended-chain growth models are considered. The first, called A, involves a straightforward surface nucleation treatment of the growth rate of an isolated "leading" lamella where the effect of the end (methyl group) surface free energy σ' on the substrate completion process is considered in detail for a pure compound where the end surface is smooth. Then an extension of this model, denoted B, is given that highlights some of the phenomena that will occur for impure *n*-paraffins or polymer fractions growing as isolated lamellae where the "methyl group" end surface is rough because of the polydispersity. The polydispersity leads to important effects in the melting behavior and the estimation of σ. Then a model denoted C is given for the case where the growth front in a pure compound is notched or troughlike as in "polytypic" crystals so that any effect of σ' on substrate completion is greatly reduced or eliminated with the result that T_0 is very close to T_m.

All of the models are worked out for two cases, namely, regime I, where one surface nucleus causes completion of the substrate of length L, so that $G \propto i$, and regime II, where multiple nucleation occurs on the substrate so that $G \propto i^{1/2}$. Here G is the growth rate and i is the surface nucleation rate. All of the models give a growth law of the form $G = K(T_0 - T)$ sufficiently near the melting point, but K and hence σ depend on the regime. The quantity T_0 is much further below T_m or $T_d°$ for model B than for models A and C. The case of C-94 crystallized from the melt can be treated with either the regime I or regime II versions of models A or C, with essentially identical results being found for σ. Model B, with its low T_0, is relevant to the case of polymer fractions. The fraction C-207 crystallized from solution proves to be a regime I case of model B and clearly brings out the effects associated with polydispersity. Rough estimates are given of the substrate length $L = n_s a_0$ and of the preexponential factor C_0 that are needed to estimate σ. The Lauritzen Z test will be adapted to extended-chain systems and used to determine the growth regime.

Model A (Version for Isolated Lamella of Pure Compound). The model is shown in Figure 1. The "lead" lamella is isolated; i.e., the growth front of the monolayer crystal is surrounded by the melt. The surface nucleation

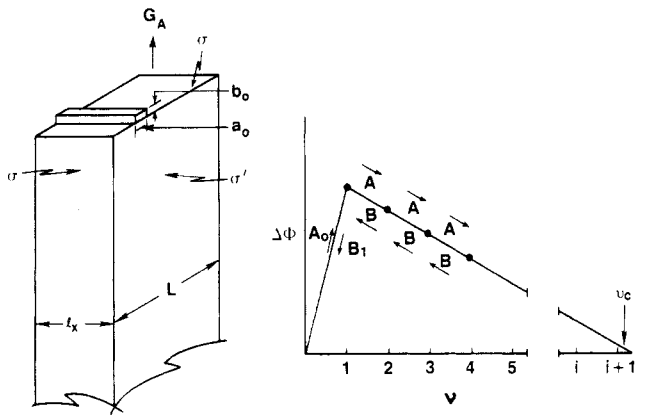

Figure 1. Model A. Growth of isolated extended-chain lamella by coherent surface nucleation mechanism. Model B is similar, except the σ'-type surface is rough as a result of the distribution of lengths that are involved in polydisperse fractions and impure compounds.

process begins when a stem of length l_x attaches to the bare σ-type surface. The stem has a lateral surface free energy σ and an end surface free energy σ'. The symbol a_0 represents the molecular width, and b_0 the layer thickness. The number of contiguous stems forming the surface patch on the substrate is denoted by ν. The first stem requires the most net free energy, which is the positive quantity $2b_0l_x\sigma + 2a_0b_0\sigma' - a_0b_0l_x(\Delta f)$ corresponding to $\Delta\phi_{\nu=1}$. Substrate completion begins when new stems attach at the niche created by the first. In the substrate completion process ($\nu \geq 2$), the net gain in stability is $a_0b_0[2\sigma' - l_x(\Delta f)]$ as $\nu_i \rightarrow \nu_{i+1}$. The overall substrate length is L. Estimates will in due course be given for L.

The free energy of formation of the surface patch is

$$\Delta\phi_\nu = 2b_0l_x\sigma + 2a_0b_0\sigma' - a_0b_0l_x(\Delta f) + (\nu - 1)a_0b_0[2\sigma' - l_x(\Delta f)] \quad (5)$$

where Δf is given by eq 2. It is already clear from eq 5 that substrate completion cannot take place, i.e., $\Delta\phi_\nu$ cannot become negative, unless $l_x(\Delta f) > 2\sigma'$. The barrier system implied by eq 5 is shown in Figure 1.

We now set down the rate constants A_0, B_1, A, and B shown in Figure 1 that are relevant to calculating the net rate of passage over the barrier. We have

$$A_0 = \beta_g e^{-2b_0\sigma l_x/kT - 2a_0b_0\sigma'/kT} \quad (6)$$

$$B_1 = \beta_g e^{-a_0b_0l_x(\Delta f)/kT} \quad (7)$$

for the forward and backward rates for the first stem, and

$$A = \beta_g e^{-2a_0b_0\sigma'/kT} \quad (8)$$

$$B = \beta_g e^{-a_0b_0l_x(\Delta f)/kT} \quad (9)$$

for the substrate completion processes. The quantity β_g represents the retardation related to the necessity of transporting the molecules in the melt to the crystal surface and we assume as a first approximation that

$$\beta_g = (kT/h)e^{-Q^*/RT} \quad (10a)$$

where Q^* is the activation energy. C-94 is long enough to diffuse by the reptation mechanism in the melt, so we would interpret Q^* as the activation energy for reptation Q_R^*, which is of course also that of center-of-mass diffusion. This is close to 23 kJ mol^{-1} or 5500 kcal mol^{-1} for n-paraffins both above and below C-94 in chain length.[9] While we shall use eq 10a in most of what follows to keep expressions simple, the expression[2]

$$\beta_g = (\kappa/x)(kT/h)e^{-Q^*/RT} \quad (10b)$$

will be used in the final calculations for C-94. Here κ is a numerical constant, and x is the number of CH_2 units in the chain. This "calibrated" modification of eq 10a is based on the reptation model[2] where the friction coefficient is proportional to $1/x$. The factor $\kappa \sim 10$ gives the same absolute value of β_g as the friction coefficient approach[2] when $Q^* = 5500$ cal mol^{-1}. Note that eq 6–9 are consistent with eq 5 and also with the principle of detailed balance.

The flux across the barrier is given by the exact relation[10]

$$S = S(l) = N_0A_0(A - B)/(A - B + B_1) \quad (11)$$

The surface nucleation rate i is defined as

$$i \equiv S/L \quad (12)$$

where L is the substrate length

$$L = n_sa_0 \quad (13)$$

in which a_0 is the width of a stem and n_s the number of stems in the substrate. We shall take L and therefore n_s to be a constant. The quantity N_0 is the number of reacting species, and we shall assume, as has been done elsewhere,[2] that N_0 is proportional to n_s as

$$N_0 = C_0n_s \quad (14)$$

where C_0 is a numerical constant. Numerical estimates of C_0 and n_s will be given subsequently.

For regime I growth, where one nucleation act causes completion of the substrate L, the growth rate is defined as

$$G \equiv b_0iL \quad (15)$$

which leads with eq 11 and 12 to

$$G = b_0S = b_0N_0A_0(A - B)/(A - B + B_1) \quad (16)$$

It follows from eq 6–9, 10a, and 16 that the growth rate for model A in regime I is

$$G_A' = N_0b_0\beta_g e^{-2b_0l_x\sigma/kT}e^{-2a_0b_0\sigma'/kT}[1 - e^{-W(T_0-T)}] \quad (17)$$

where we have set

$$\Delta T_0 = T_m - T_0 = 2\sigma'T_m/l_x(\Delta h_f) \quad (18)$$

Thus, for model A, the crystallization temperature must fall below T_0, which is below T_m, before crystallization can begin. This results from the inclusion of the end surface free energy σ' in the substrate completion calculations and arises directly from the factor $A - B$ in eq 11. In the case of small effective undercoolings $T_0 - T$, the exponential in brackets in eq 17 can be expanded to yield

$$G_{A'(T\leq T_0)} = K_A'(T_0 - T) \quad (19a)$$

where

$$K_A' = N_0b_0(kT/h)We^{-(2b_0l_x\sigma/kT)-(2a_0b_0\sigma'/kT)-Q^*/RT} \quad \text{(regime I)} \quad (19b)$$

and

$$T_{0(A)} = T_m\{1 - 2\sigma'/\Delta h_fl_x\} \quad (19c)$$

In eq 17 and 19b

$$W = a_0b_0l_x(\Delta h_f)/(kT)T_m \quad (20)$$

This quantity, which is roughly 0.5 deg^{-1} for the n-hydrocarbons of interest here, will appear repeatedly in this work.

Observe that the factor $T_0 - T$ in eq 19a arises directly from the temperature dependence inherent in the substrate completion process as expressed as $A - B$ in eq 11. The growth rate will depart from eq 19a at large values of T_0

$- T$. Because σ' is probably quite small for a pure compound, one may expect the factor $\exp(-2a_0b_0\sigma'/kT)$ in eq 17 and 19 to be the order of unity for pure materials. Similarly, $T_{0(A,)}$ in eq 19c will be quite close to T_m.

The rate expressions eq 6–9 above correspond[1,11] to the case $\psi = 0$. If the general case for ψ is worked out, K_A contains an extra factor of the form $\exp[\psi a_0b_0l_x(\Delta f)/kT]$. This has no important effect at low ΔT and does not affect the value of σ to be given later for C-94. It can be important at large undercoolings, as will become evident in the more exact treatment of C-207 with model B. The expression for K for model C also contains this factor.

We note that the detailed calculations of the growth flux for C-24 and C-26, and mixtures thereof, by Lauritzen, Passaglia, and DiMarzio[12] using the LDP[13] formalism indicate that G in regime I varies almost exactly as ΔT in the region where ΔT is small. Thus, our simpler version of surface nucleation-controlled growth in regime I in chain systems agrees with this detailed analysis on this important point. Their treatment was arranged to that the T_0 effect did not appear.

We now give the growth rate for regime II, in which multiple nucleation occurs on the substrate. For regime II[14,15]

$$G'' \equiv b_0(2ig)^{1/2} \tag{21}$$

Here i is S/L as before. The substrate completion rate is[1,2]

$$g = a_0(A - B) \tag{22}$$

Hence with eq 11–14 and the expressions just given

$$G'' = b_0(A - B)(2C_0)^{1/2}[A_0/(A - B + B_1)]^{1/2} \tag{23}$$

With the rate constants given in eq 6–9 it is readily deduced at low values of $T_0 - T$ that

$$G_A''_{(T\le T_0)} = K_A''(T_0 - T) \tag{24a}$$

where

$$K_A'' = (2C_0)^{1/2}b_0(kT/h)We^{-b_0l_x\sigma/kT}e^{-2a_0b_0\sigma'/kT}e^{-Q^*/RT} \quad \text{(regime II)} \tag{24b}$$

Thus, regime II at small $T_0 - T$ leads to a growth law identical in general form with regime I with regard to the dependence of the growth rate on undercooling. Equation 19c still holds for T_0. The most notable difference from regime I is the absence of L or n_s, and the loss of a factor of 2 in the exponential involving σ (compare eq 19b and 24b). As in the case of regime I, the factor $T_0 - T$ in G_A'' arises from $A - B$.

The double prime is used in eq 24, and in expressions to be given subsequently, to denote regime II; a single prime denotes regime I.

The results given in eq 19 and 24 apply to the case where the "leading" lamella that precedes all ensuing crystallization is isolated; i.e., it is a monolayer crystal where the growth front is surrounded by the melt.

The treatment given above for an isolated "lead" lamella does not exhaust the possibilities for nucleation-controlled crystallization in a pure extended-chain compound. The quantity ΔT_0 is very small ($\sim$0.039 °C) in C-94, and this could be a result of σ' in eq 19c being sufficiently small in an isolated lead lamella. Possibly σ' in a pure compound is small enough to accommodate such a small ΔT_0, but it seems reasonable to examine other models where ΔT_0 is inherently small. It is in any case not necessary to require that the growth front for a pure compound must consist of an isolated lamella. Certainly the final crystal produced by melt crystallization in C-94 is multilamellar; i.e., n_l is large. There is evidence, to be cited later, that the leading lamellae are sometimes associated with a troughlike growth front as in so-called "polytypic" crystals, and this multilamellar "notched" front leads naturally to a very small effective value of σ' and therefore a very small ΔT_0. This case will be treated as model C. Models A and C are in important respects similar and lead to nearly identical values of σ for C-94. Meanwhile we shall introduce a version of model A, called B, that shows in an approximate manner what must be expected for a quite impure n-paraffin or a polydisperse polyethylene fraction such as C-207 with a rough σ'-type end surface that grows as an isolated extended-chain lamella.

Model B (Version for Isolated Lamella, Impure Compound or Polydisperse Fraction). We suppose the specimen to have a distribution of lengths about $\bar{l}$ such that the shortest of the molecules that can engage in nucleation or substrate completion is

$$l_{min} = \bar{l}(1 - \gamma) \tag{25}$$

where γ is perhaps 0.1–0.2. This model immediately requires that the σ'-type surface be rough because of the distribution of lengths. It also brings out the point that in a fraction a molecule of length l_{min} will be involved in nucleating the first stem. Below we examine the consequences of these effects. This model will prove to be particularly useful since it is known that the polymer fraction we have designated as C-207 crystallizes in the extended-chain form from solution as an isolated lamella.

In this model it is useful to distinguish the end surface free energy associated with the first stem, which we will call σ_1', from the end surface free energy associated the substrate completion process which we still call σ'. The rate expressions, in which we now regard the chain length l as a variable whose lower bound is $\bar{l}(1 - \gamma)$, are as follows:

$$A_0 = \beta_g e^{-pl}e^{-2a_0b_0\sigma_1'/kT} \tag{26}$$

$$B_1 = \beta_g e^{-ql} \tag{27}$$

$$A = \beta_g e^{-2a_0b_0\sigma'/kT} \tag{28}$$

$$B = \beta_g e^{-ql} \tag{29}$$

Here $p = 2b_0\sigma/kT$, $q = a_0b_0(\Delta f)/kT$, and $T_{0(B)} = T_m\{1 - 2\sigma'/\Delta h_f\bar{l}\}$. It follows that the total flux is[1]

$$S_T = (1/l_u)\int_{l=\bar{l}(1-\gamma)}^{\infty} N_0A_0[(A - B)/(A - B + B_1)]\,dl \tag{30}$$

We find for the case where an isolated lamella grows from a melt containing a distribution of lengths that for regime I where $G \equiv b_0iL = b_0S_T$

$$G_B' \cong N_0b_0\beta_g e^{-2b_0\sigma\bar{l}(1-\gamma)/kT}e^{-2a_0b_0\sigma_1'/kT}[1 - e^{-W(T_0-T)}] \tag{31}$$

where we have set a factor of $kT/2b_0\sigma l_u$ equal to unity and let the quantity $r = a_0b_0(\Delta h_f)(T_0 - T)/kTT_m$ be much less than p. On expansion of the exponential in brackets we have for very low $T_0 - T$

$$G_B'_{(T\le T_0)} = K_B'(T_0 - T) \tag{32a}$$

where

$$K_B' \cong N_0b_0(kT/h)We^{-2b_0\sigma\bar{l}(1-\gamma)/kT}e^{-2a_0b_0\sigma_1'/kT}e^{-Q^*/RT} \quad \text{(regime I)} \tag{32b}$$

Note that

$$T_{0(B)} = T_m\{1 - 2\sigma'/\Delta h_f\bar{l}\} \tag{32c}$$

For the case of regime II, where multiple nucleation occurs and $G'' = b_0(2ig)^{1/2}$, one finds using eq 23 with $i \equiv S_T/L$ and $g = a_0(A - B)$ that for small values of $T_0 - T$

$$G_B''_{(T \le T_0)} = K_B''(T_0 - T) \quad (33a)$$

where

$$K_B'' \cong (2C_0)^{1/2} b_0 (kT/h) W e^{-b_0 \sigma \bar{l}(1-\gamma)/kT} e^{-2a_0 b_0 \sigma_1'/kT} e^{-Q^*/RT} \quad \text{(regime II)} \quad (33b)$$

Thus, the general form of the growth law derived for regime I at very low undercoolings has been preserved in regime II, but neither n_s nor L appears, and a factor of 2 has been lost in the exponent involving σ. Equation 32c holds for regime II. In what follows, we shall let $\bar{l} = l_x$, where l_x is calculated from the number-average molecular weight.

Though they can be employed to estimate $\sigma(1 - \gamma)$ with reasonable accuracy, the equations given so far for model B cannot be used to predict $G(T)$ at larger $T_0 - T$, partly because the expansion of the exponential involving $T_0 - T$ is then invalid as a source for a factor of $T_0 - T$ in $G(T)$, and partly because fitting data at large $T_0 - T$ involves the value of ψ.[11] We shall subsequently deal with growth rate data on C-207 over a considerable range of $T - T_0$ in the extended-chain region. Since C-207 in the extended-chain region will prove to be a regime I case, we give the more exact expression for the growth rate in this regime with the functionality of both ψ and γ included:

$$G_B' = C_0 n_s b_0 (kT/h)\{[1 - e^{-W(T_0-T)}] e^{\psi^* W(T_0-T)} e^{2\psi^* a_0 b_0 \sigma'/kT}\} e^{-Q^*/RT - 2b_0\sigma((1-\gamma)l_x)/kT} \quad \text{(regime I, all } T_0 - T\text{)} \quad (33c)$$

where

$$\psi^* = \psi(1 - \gamma) \quad (33d)$$

This was derived for small γ by using eq 16 and the definitions of A_0, B_1, A, and B given in footnote 11 under the condition $\sigma_1' \to 0$. Observe that for the case $\psi = 0$, eq 33c reverts to eq 31 with $\sigma_1' = 0$. At low $T_0 - T$, the $G \propto T_0 - T$ law is associated almost exclusively with the behavior of the substrate completion process as expressed by $1 - \exp[-W(T_0 - T)]$, but at large $T_0 - T$ this law persists partly because of the increase of the primary nucleation rate caused by the factor $\exp[\psi^* W(T_0 - T)]$. For appropriate values of ψ^*, which are in the vicinity of $\sim 1/2$, a growth law closely approximating the form $G_B' \propto T_0 - T$ is preserved by eq 33c over the entire range of extended-chain growth for C-207. (We note here that in the most general case, deviations from $G \propto T_0 - T$ are to be anticipated at sufficiently large $T_0 - T$.) Highly accurate $\sigma(1 - \gamma)$ and ψ^* values can be obtained by fitting the data (see later). An empirical multiplying factor of c^α where c is the weight percent concentration of polymer and $\alpha \cong 0.4$ has been omitted in eq 33c, but will be inserted in dealing with C-207 crystallizing from dilute solution.

Model B illustrates some important points. First, it is clear from the treatment that a molecule near $l_{min} = l_x(1 - \gamma)$ will be involved in nucleating the first stem. This has the important consequence that the "σ" arrived at by analyzing data on fractions is actually $\sigma(1 - \gamma)$; i.e., it is lower than the true σ. It is emphasized that l_{min} represents one of the shorter molecules in the distribution that can still crystallize at a given undercooling: it does *not* represent the length of the smallest molecule actually present in the distribution. A very short molecule has a correspondingly small free energy of fusion, as shown by eq 3, and will not crystallize. For a material such as C-207, we would suppose that γ might well lie in the range of 0.1–0.2 (see later). The uncertainty concerning the exact value of γ will emerge as the main source of error in estimating σ for C-207.

Another point is that one must expect a considerably enhanced value of σ' in the substrate completion process because of the inherent roughness of the end surface resulting from the distribution of lengths in a fraction of impure compound. A crude model will illustrate this point. Even a short protruding stem will expose its lateral or σ-type surface, which will then act locally as a large effective end surface free energy σ'. If the average roughness of the end surface is only two chain units, the effective value of σ' would be $\sim 4\sigma l_u(a_0 + b_0)/a_0 b_0$, which with $\sigma =$ 10 erg cm^{-2} already comes to $\sigma' \sim$ 23 erg cm^{-2} for the paraffin system. Longer cilia with a random-coil natural will contribute even more to σ'. Because of the inherent σ' surface roughness, we expect through eq 32c that T_0 will be significantly below T_m or $T_d°$ for polydisperse fractions or highly impure compounds. In due course we shall cite an example where T_0 for an isolated extended-chain lamella of a polyethylene fraction crystallized in dilute solution has a T_0 many degrees below the equilibrium dissolution temperature $T_d°$, and which obeys a $G_B' = K(T_0 - T)$ law below T_0. The quantity σ_1' in eq 32b, 33b, and 33c will likely be much less than the average σ' for the complete substrate, since the first stem will tend to be slightly shorter than $\bar{l}$ and therefore not protrude as a cilium from the previously established σ'-type surface.

Model B is especially clear on the point that the extrapolation of the growth rate to zero is not always a proper criterion for determining the melting point, if by "melting point" one means the T_m or $T_d°$ associated with a multilayered crystal with large n_l. Such an extrapolation gives T_0, which is the melting point of an isolated lamella. An "annealed" specimen of the same material that is "multilayered" in the sense that chain ends from one rough-surfaced lamella have interpenetrated into contiguous lamellae and thus become largely localized will melt at a higher temperature, namely T_m when no solvent is present, or $T_d°$ for the case where solvent is present. The function $T_0 - T_x$ is of course the proper effective undercooling to use in analyzing the growth rates of extended-chain fractions with rough end surfaces, and not $T_m - T_x$ or $T_d° - T_x$. This is sometimes an important distinction. The thermodynamic driving force Δf is always measured from T_m or $T_d°$, and not T_0.

Finally, it is of interest to note that model B for the case $\gamma = 0$, $\psi = 0$, $\sigma_1' = \sigma'$ becomes identical with model A for each regime. In this sense, model B represents the more general case.

Model C (Pure Compounds with Notched Growth Front). There is evidence that shows that certain pure n-paraffins of highly uniform chain length grow from dilute solution as polytypic crystals where the growth front is notched or troughlike as shown schematically in Figure 2. This is particularly clear in the studies of Aquilano on C-28 from solution[16] (see especially his Figure 2). Growth fronts of the type shown schematically in Figure 2 appear to be associated with the lateral growth rate G_C of such crystals. While there is no direct evidence that the growth front is notched in this manner in the crystallization of C-94 from the melt, we shall proceed on the basis that it might occur. In model C the chain molecules add onto a substrate that is essentially part of a trough. This brings about a situation where there is either no (or at any rate very little) net new σ' surface formed as a stem attaches to the substrate. The situation is altogether analogous to the fact that in the substrate completion process no new σ-type surface is formed when a stem attaches to a niche. Here we will let

$$\sigma' - \epsilon = \Delta\sigma' \quad (34)$$

where $-\epsilon$ is the attraction energy for the CH_3 group in the trough and σ' the normal end-group surface free energy. We expect $\Delta\sigma'$ to be very small in a notched system. By

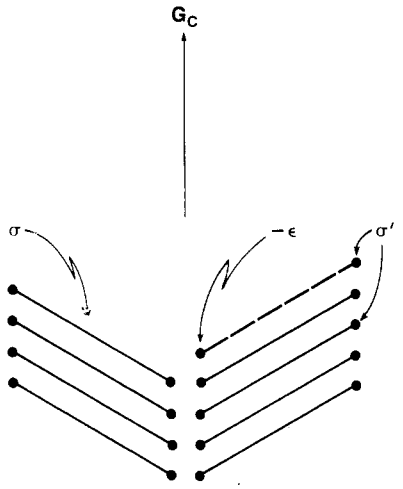

Figure 2. Model C. Troughlike "notched" growth front in extended-chain polytypic crystal (schematic). Dashed line represents first ($\nu = 1$) stem beginning new layer.

the same procedures used before, we have for the free energy of formation of the surface patch

$$\Delta\phi_\nu = 2b_0 l_x\sigma + a_0b_0(\Delta\sigma') - a_0b_0l_x(\Delta f) + (\nu - 1)a_0b_0[\Delta\sigma' - l_x(\Delta f)] \quad (35)$$

from which it is apparent that substrate completion can take place only when $l_x(\Delta f) > \Delta\sigma'$, which in turn implies that crystallization can occur at very low undercoolings. Formally, the barrier system is the same as shown in the diagram in Figure 1, but the rate constants A_0 and A are revised to

$$A_0 = \beta_g e^{-2b_0l_x\sigma/kT}e^{-a_0b_0(\Delta\sigma')/kT} \quad (36)$$

$$A = \beta_g e^{-a_0b_0(\Delta\sigma')/kT} \quad (37)$$

The rate constants B_1 and B are the same as those for model A. Inserting these into eq 16 gives for regime I

$$G_C' = N_0b_0\beta_g e^{-2b_0\sigma l_x/kT}e^{-a_0b_0(\Delta\sigma')/kT}[1 - e^{-W(T_0-T)}] \quad (38)$$

which leads for small values of $T_0 - T$ (say 0.5 °C or less) to

$$G_C'_{(T\le T_0)} = K_C'(T_0 - T) \quad (39a)$$

where

$$K_C' = N_0b_0(kT/h)We^{-2b_0\sigma l_x/kT}e^{-Q^*/RT} \quad \text{(regime I)} \quad (39b)$$

Here

$$T_{0(C)} = T_m\left\{1 - \frac{(\Delta\sigma')T_m}{l_x(\Delta h_f)}\right\} \quad (39c)$$

For the case of regime II, model C yields at low $T_0 - T$ the expected relation

$$G_C''_{(T\le T_0)} = K_C''(T_0 - T) \quad (40a)$$

where

$$K_C'' = (2C_0)^{1/2}b_0(kT/h)We^{-b_0\sigma l_x/kT}e^{-Q^*/RT} \quad \text{(regime II)} \quad (40b)$$

The exponential factor involving $\Delta\sigma'$ in eq 39b and in eq 40b is set equal to unity in anticipation that $\Delta\sigma'$ is very small, which is clearly justified in the case of C-94. Through eq 39c both regime I and regime II versions of model C allow T_0 to be very near T_m even when σ' is greater than zero and even has a value comparable to σ.

Estimate of Substrate Length L and C_0: The Crystallization Regime and the Lauritzen Z Test. It is seen from the foregoing that we shall require an estimate of the substrate length $L = n_s a_0$ in order to analyze growth rate data in regime I to obtain σ, since the absolute value of σ depends on $N_0 = C_0n_s$. An order-of-magnitude estimate for L or n_s will suffice, since σ will prove to be quite insensitive to even large changes in N_0. For regime II growth, it is required to have an order-of-magnitude estimate of C_0 to calculate σ. Estimates of C_0 and n_s are also needed for the Z test that determines the regime to be discussed below.

A reasonable lower bound for n_s can immediately be established. The quantity n_s cannot be less than the number of stems that correspond to a stable surface nucleus. To determine this, we find the number of stems ν_c where the strip formation process allows the free energy of formation to fall to zero (Figure 1). Thus, we set expressions of the form of eq 5 or 35 equal to zero and note that $T_0 = T_m[1 - 2y/\Delta h_f l_x]$ where $y = \sigma'$ or $\Delta\sigma'$ to find

$$\nu_c = n_{s(min)} \cong 2\sigma T_m/a_0(\Delta h_f)(T_0 - T) \quad (41)$$

L_{min} is given by $a_0n_{s(min)}$.

The above expression demands very large values of L for C-94 near the melting point. To anticipate, growth rate measurements were actually made on C-94 at a $T_0 - T$ of 0.006 °C. If we use this figure with $\sigma \sim 10$ erg cm^{-2}, $T_m = 386.63$ K, $a_0 = 4.55 \times 10^{-8}$ cm, and $\Delta h_f = 2.8 \times 10^9$ erg cm^{-3}, it is found with eq 41 that $n_{s(min)} \cong 10^4$, corresponding to $L_{(min)} \sim 4.6$ μm. The actual value of L would have to be larger, and in the illustrative calculations assuming regime I for C-94 to follow we use $L = 15$ μm, corresponding to $n_s = 3.3 \times 10^4$. This estimate of L is comparable to the observed size of the growth front in C-94 at $T_0 - T = 0.006$ °C (see later).

For C-207, because of the much larger $T_0 - T$ values involved, one finds no serious restrictions on the lower bound of n_s. In this case, we choose a value of L of 1 μm. This is smaller than the largest straight-edged faces (~3–5 μm) on the diamond-shaped extended-chain crystals, and comparable to the L value for polyethylene.

Comment is required on the estimates of C_0 that will be employed in the calculations.

The lowest possible value of C_0 is unity, which corresponds to the undoubtedly oversimplified case where the number of reacting species $N_0 = C_0n_s$ is taken to be n_s, the number of stems on the substrate. The simplest theoretical prediction for C_0 would be $C_0 \cong x$, where x is the number of CH_2 units in a single stem, thus giving $N_0 = xn_s$ as the number of CH_2 units in the surface. From studies on polyethylene fractions, where the presence of regime I → II transitions permitted it to be estimated, C_0 was found[2] to be between about 5×10^2 and 10^4. (A recent as yet unpublished reanalysis of the original data carried out for another purpose affirms the range of values just cited.) In this paper we shall use C_0 values ranging from 10 to 10^4. In our view this covers the entire range of reasonable values.

The Lauritzen Z parameter has the definition[14] given in the first equality in

$$Z \equiv iL^2/4g = (C_0n_s^2/4)[A_0/(A - B + B_1)] \quad (42a)$$

The right-hand side is derived from eq 11–14 and 22. If $Z \le 0.1$, the system is crystallizing in regime I, and if $Z \ge 1$, the crystallization is in regime II. A value of $Z \sim {}^1/_2$ indicates "mixed" regime I and II. In the instance of C-94 where σ' is small and ΔT very small, the relation

$$Z = (C_0n_s^2/4)e^{-2b_0\sigma l_x/kT} \quad (42b)$$

Table I
Growth Rates of C-94 from the Melt

T_x,[a] °C	$T_m - T_x$,[b] °C	growth rate, cm s^{-1}	$T_0 - T_x$,[c] °C
113.424	0.045	2.61×10^{-6}	0.006
113.413	0.056	5.65×10^{-6}	0.017
113.397	0.072	1.81×10^{-5}	0.033
113.388	0.081	2.48×10^{-5}	0.042
113.372	0.097	2.88×10^{-5}	0.058
113.325	0.144	4.83×10^{-5}	0.105
113.310	0.159	5.45×10^{-5}	0.120
113.172	0.297	1.38×10^{-4}	0.258
113.172	0.297	1.20×10^{-4}	0.258

[a] Crystallization temperature. [b] Undercooling. T_m = 113.469 °C as actually measured on hot stage. [c] Effective undercooling. Calculated by using $T_m - T_0$ = 0.039 °C, or T_0 = 113.430 °C.

is an excellent approximation. Because of the small undercooling involved, Z does not depend to a significant extent on ψ. In the case of C-207, σ' is quite large, as is the undercooling ΔT. For this situation one readily finds that an expression of sufficient accuracy is

$$Z = (C_0 n_s^2/4)\{e^{2a_0 b_0 \sigma'/kT} e^{-\psi\gamma W(\Delta T)}\} e^{-2b_0\sigma(1-\gamma)l_x/kT} \quad (42c)$$

With the information given above concerning C_0 and n_s, and with the values of σ (or $\sigma(1-\gamma)$) to be obtained shortly, it is possible to give precise statements concerning the regime of crystallization for C-94 and C-207. The identification of the regime in each case is quite certain, since large variations in C_0 and L (i.e., n_s) do not alter the outcome. As will be seen, C-94 represents a mixed regime I and II case, while C-207 will prove to be a good example of regime I crystallization.

III. Experimental Data for C-94

The experimental procedure outlined below is that of Ross and Ross.[17] The C-94 used in this investigation was originally prepared at the Pennsylvania State University for Dr. E. Passaglia, then of the American Viscose Corp., and later zone-refined by Dr. John Crissman of the National Bureau of Standards. From melting point studies, it was estimated that the sample was ca. 99.9 mol % pure. The actual melting point was 113.469 °C as was repeatedly observed in the microscope hot stage. The melting point extrapolated to 100 mol % purity was 113.478 °C. Hence, the melting point depression resulting from impurities was only ~0.11 °C. Crystallization rate experiments were carried out in a special oil bath hot stage that could be controlled to within ±0.001 °C for up to several hours. This accuracy was required because of the narrow range of temperature in which growth rates could be observed. The sample was about 10–40 μm thick and confined between ultrasonically cleaned microscope cover slips. The cover slip–sample assembly was immersed in the silicone oil bath on the hot stage, and the sample very nearly completely melted to form "seeds". The stage was then cooled to the desired growth temperature and the rate of crystal growth determined from optical micrographs (crossed polarizers) or sometimes with a calibrated eyepiece. The growth rate was constant with time when the crystals were of small or moderate size, but sometimes fell off when the crystals became large. In such cases, only initial growth rates are reported. At low undercoolings (ΔT ~ 0.05–0.07 °C) the crystal were frequently needlelike, and occasionally rhomboid. In the case of asymmetric crystals, the largest dimension was used in determining G. These crystals usually appeared to have faceted growth tips, but the rhomboid type often exhibited curved edges. The growth front was as large as ~5–15 μm at very low undercoolings. At high undercoolings (ΔT ~ 0.16–~0.3 °C) the crystals had a much finer texture and resembled spherulites. The results for the nine runs in which the investigators had the most confidence are given in Table I and plotted in Figure 3. This selection was based mainly on the quality of the temperature control for each run as determined by frequent measurements with an accurately calibrated thermocouple situated close to the field of view.

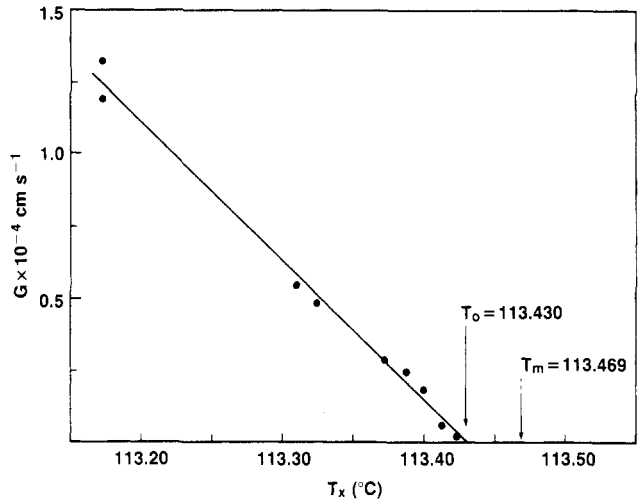

Figure 3. Growth rate of C-94 extended-chain crystals from the melt as a function of isothermal crystallization temperature. Slope $K = 4.855 \times 10^{-4}$ cm s^{-1} deg^{-1}. From this slope it is determined that σ = 13.8 ± 2.1 erg cm^{-2}.

Khoury[18] has shown that C-94 crystallizes from the melt with monoclinic II_m unit cell, which is closely related to the orthorhombic I_0 unit cell that appears from dilute solution. Both possess the same orthorhombic subcell, a_s = 7.4 Å, b_s = 4.95 Å, c_s = 2.54 Å. Surface replicas of the growth front of the melt-crystallized material reveal a distinctly stepped surface structure of the order of 100 Å, which coincides with the (001) spacing of the II_m unit cell. While the stepped feature of the replicas for melt-crystallized C-94 seems consistent with the troughlike growth front shown schematically in Figure 2 for model C, it cannot be stated with certainty that melt-crystallized C-94 grows in the polytypic mode.

IV. Analysis of Results for C-94 Crystallized from the Melt

Critical Undercooling ΔT_0. It is seen in Figure 3 that the growth rate goes to zero below T_m. Also $G \propto T_0 - T$ below T_0 as suggested by the theory for models A and C.

It is readily found from the data that

$$G\ (\text{cm s}^{-1}) = -1.900 \times 10^{-5} + 4.855 \times 10^{-4}(T_m - T) \quad (43a)$$

or

$$G\ (\text{cm s}^{-1}) = 4.855 \times 10^{-4}(T_0 - T) \quad (43b)$$

where T_m = 113.469 °C, T_0 = 113.430 °C, and ΔT_0 = 0.039 °C. This means that

$$K_{\text{exptl}}\ (\text{cm s}^{-1}\ \text{deg}^{-1}) = 4.855 \times 10^{-4} \quad (44)$$

The correlation coefficient for the fit is 0.996. Because of the accuracy of the temperature control, and the rather small error in the growth rates, there is good reason to believe that the critical undercooling effect, where T_0 falls below T_m, is real (Figure 3).

The low value of $T_m - T_0 = \Delta T_0$ = 0.039 °C can be explained in at least two ways. One could use model A, in which case it is found with eq 19c that σ' for an isolated

lamella using $l_x = 94 \times 1.27 \times 10^{-8} = 1.194 \times 10^{-6}$ cm and $\Delta h_f = 2.8 \times 10^9$ erg cm^{-3} is

$$\sigma'(\text{model A}) \cong 0.17 \text{ erg cm}^{-2} \quad (45)$$

It could also be assumed that the "notch" model applied, in which case it is found with eq 39c that

$$\Delta\sigma'(\text{model C}) \cong 0.34 \text{ erg cm}^{-2} \quad (46)$$

It is not possible to make a decision concerning which explanation is correct. We would offer even a third possible explanation of the very small ΔT_0. If a small fraction of the molecules had a chain length differing from C-94—say one or two in a thousand—the few protruding stems could give a T_0 just below T_m as for a limiting case of model B. Such an explanation implicitly assumes that σ' for an ultrapure specimen of C-94 is very nearly zero. For the present, we are inclined to favor model C, partly because of the work of Aquilano[16] on C-28. This allows σ' to be comparable to σ but gives T_0 very close to T_m. None of the above explanations raise any serious issue regarding our main purpose, however, since once the value of T_0 is established, the experimental value of K and hence σ can be obtained without further reference to the quantities that determine T_0.

Estimate of σ from K_{exptl} (Models A or C). For regime I we have with $N_0 = C_0 n_s$ for models A or C by eq 19b or 39b

$$2b_0\sigma l_x/kT = \ln (C_0 n_s) - \ln K_{A,C} + \ln (\kappa/x)\{a_0 b_0^2 l_x(\Delta h_f)/hT_m\} - Q^*/RT - 2a_0 b_0 \sigma'/kT \quad (47)$$

The term involving σ' is included for model A only. The corresponding factor involving $\Delta\sigma'$ for model C may safely be taken as zero.

Here we have replaced kT/h from eq 10a with $(\kappa/x)\cdot(kT/h)$ from eq 10b with $\kappa = 10$ and $x = 94$. This is the better choice for a system where diffusion in the melt takes place by reptation. With $b_0 = 4.15 \times 10^{-8}$ cm, $l_x = 94 \times 1.27 \times 10^{-8} = 1.194 \times 10^{-6}$ cm, $T_m = 386.63$ K, $a_0 b_0 = 18.9 \times 10^{-16}$ cm^2, and $\Delta h_f = 2.8 \times 10^9$ erg cm^{-3}, the quantity in brackets comes to 1.024×10^5 cm s^{-1} deg^{-1}. Then with $K_{A,C} = K_{exptl} = 4.855 \times 10^{-4}$ cm s^{-1} and $Q^* = 5500$ cal mol^{-1}, which is appropriate[9] to the liquid n-alkanes both considerably longer and shorter than C-94, eq 47 reduces to

$$\sigma \text{ (erg cm}^{-2}) = 5.26 + 0.538 \ln (C_0 n_s) - 3.8 \times 10^{-2}\sigma' \quad \text{(regime I)} \quad (48)$$

The term involving σ' applies only to model A in eq 48 and 49.

The corresponding expression for regime II for models A or C as derived from eq 24b or 40 is

$$\sigma \text{ (erg cm}^{-2}) = 10.9 + 0.538 \ln C_0 - 7.6 \times 10^{-2}\sigma' \quad \text{(regime II)} \quad (49)$$

The results of the calculations for C-94 with eq 48 and 49 are shown in Table II. Application of the Lauritzen Z test using eq 42b with the σ values in this table gives Z values of $\sim^1/_2$ for both regimes I and II. Crystallization is therefore clearly mixed regime I and II in the case of C-94. It is seen in the regime I results that a large variation in N_0 causes but little change in σ and that the effect of an end surface free energy σ' is minimal. The effect of large changes of C_0 for regime II is small, and the effect of σ' negligible. It is seen for C-94 that there is little to choose between the regime I and regime II results. This would hold even for assumed substrate lengths 1 order of magnitude different from $L = 15$ μm. As the Lauritzen Z test shows, this is a mixed-regime case, and it is evident that this does not alter the value of σ in a significant manner. The value $\sigma = 13.8 \pm 2.1$ erg cm^{-2} brackets all the calculated results for both regimes, and we take this to be the lateral surface free energy for C-94. Because of the low value of $T_0 - T$, this result is completely independent of ψ.[11] No account need be taken of the effect of polydispersity in C-94.

Table II
Estimated Values of σ from Growth Rate Data on Melt-Crystallized C-94[a]

Models A or C, Regime I[b]

trial value of C_0	$10^{-4} n_s$	L,[c] μm	N_0[d]	σ by eq 48, erg cm^{-2}	
				σ' or $\Delta\epsilon = 0$[e]	$\sigma' = 5$[f]
10	3.3	15	3.3×10^5	12.10	11.91
10^2	3.3	15	3.3×10^6	13.34	13.15
10^3	3.3	15	3.3×10^7	14.58	14.39
10^4	3.3	15	3.3×10^8	15.82	15.63

Models A or C, Regime II[b]

trial value of C_0	σ by eq 49, erg cm^{-2}	
	$\Delta\epsilon$ or $\sigma' = 0$[e]	$\sigma' = 5$[f]
10	12.13	11.75
10^2	13.37	12.99
10^3	14.61	14.23
10^4	15.85	15.46

[a] $K_{exptl} = 4.855 \times 10^{-4}$ cm s^{-1} deg^{-1}; $Q^* = 5500$ cal mol^{-1}, $l_x = 1.194 \times 10^{-6}$ cm. [b] Z is found to be $\sim^1/_2$ for both regimes I and II, indicating that C-94 crystallizes in a mixed regime I and II mode. [c] Assumed substrate length. $L = a_0 n_s$. [d] $N_0 = C_0 n_s$. [e] Model A or C. [f] Model A only.

We conclude that σ in C-94 has a value centering around 13.8 erg cm^{-2} and that the growth process near the melting point is nucleation controlled. The growth type is mixed regime I and II.

V. Analysis of Extended-Chain Growth Rate Data on a Polyethylene Fraction Corresponding to C-207 Crystallized from Dilute Solution

Leung and Manley[7] have measured the rate of growth from dilute xylene solution of extended-chain lamellae of a polymer fraction (denoted 3100) whose number-average molecular weight corresponds to C-207, and where $M_w/M_n = 1.07$. This gives $\bar{l} = l_x = 2.629 \times 10^{-6}$ cm. It is certain in this case that the crystals grow as *isolated* extended-chain lamellae.[7] The crystals have a quite perfect diamond shape with 110 faces, show no sectorization, and exhibit lineal growth only.[7]

As predicted by model B for impure materials and fractions, T_0 is far below $T_d°$ (Figure 4). The $T_d°$ is 94.2 °C = 367.4 K and T_0 is 86.6 °C = 359.8 K, so ΔT_0 is 7.6 °C. This leads through eq 32c with $\Delta h_f = 2.8 \times 10^9$ erg cm^{-3} to $\sigma' \cong 76$ erg cm^{-2}. This large effective value of σ' is clearly a result of the rough, i.e., ciliated, σ'-type surface that must exist in a fraction exhibiting polydispersity, as contrasted with a pure material. This strikingly shows that the rough "end" surface in a fraction or impure material will strongly depress the melting point and crystallization onset temperature of an isolated lamella of such a crystal.[18a]

A $G = K(T_0 - T)$ law is seen in Figure 4 to be closely obeyed even down to a temperature near that where once-folded crystallization begins. The slope in the extended-chain region for a concentration of 0.05% is $K \cong 2.0 \times 10^{-8}$ cm s^{-1} deg^{-1}, which is much smaller than that for C-94.

The theoretical prediction of a law of the form $G_B = K(T_0 - T)$ for both regime I and II as we have given it earlier in eq 32a and 32b, and 33a and 33b, applies only

Table III
Estimated Values of σ from Dilute-Solution Growth Rate Data for Fraction C-207[a]

Model B, Regime I

trial value of C_0	L,[b] μm	n_s[c]	N_0[d]	exptl $\sigma(1-\gamma)$ by eq 51, erg cm^{-2}		σ,[e] erg cm^{-2}			remarks
				$\sigma_1' = 0$	$\sigma_1' = 5$	$\gamma = 0.1$	$\gamma = 0.2$	$\gamma = 0.3$	
10	1	2.2×10^3	2.2×10^4	8.12	8.03				All values of
10^2	1	2.2×10^3	2.2×10^5	8.64	8.55	**10.47**[g]	**11.78**[g]	13.46[g]	$\sigma(1-\gamma)$ shown
				(9.42; $\psi^* = 0.498$)[f]					pass regime I
10^3	1	2.2×10^3	2.2×10^6	9.15	9.06				Z test.
10^4	1	2.2×10^3	2.2×10^7	9.67	9.58	**11.67**	**13.15**	15.06	Regime I
				(10.52; $\psi^* = 0.539$)[f]					growth is clearly
10^4	5	1.1×10^4	1.1×10^8	10.04	9.95				indicated.

Model B, Regime II

trial value of C_0	$\sigma(1-\gamma)$ eq 52 erg cm^{-2}		remarks
	$\sigma_1' = 0$	$\sigma_1' = 5$	
10	12.41	12.24	All values of $\sigma(1-\gamma)$ shown fail
10^2	12.94	12.77	regime II Z test. Assumption of
10^3	13.44	13.27	regime II growth is invalid.
10^4	13.97	13.80	

[a] $K_{exptl} \cong 6.8 \times 10^{-8}$ cm s^{-1} deg^{-1}, $Q^* = 2000$ cal mol^{-1}, $\bar{l}_x = 2.629 \times 10^{-6}$ cm. [b] Assumed L. [c] $n_s = L/a_0$. [d] Resultant $N_0 = C_0 n_s$. [e] σ for various values of γ to give estimated correction for polydispersity. [f] First number in parentheses is $\sigma(1-\gamma)$ as calculated according to exact procedure outlined in eq 53 and second number is the corresponding ψ^*. [g] The numbers in these columns are based on the exact $\sigma(1-\gamma)$ values from eq 53 shown in parentheses in column at left combined with the assumed values of γ.

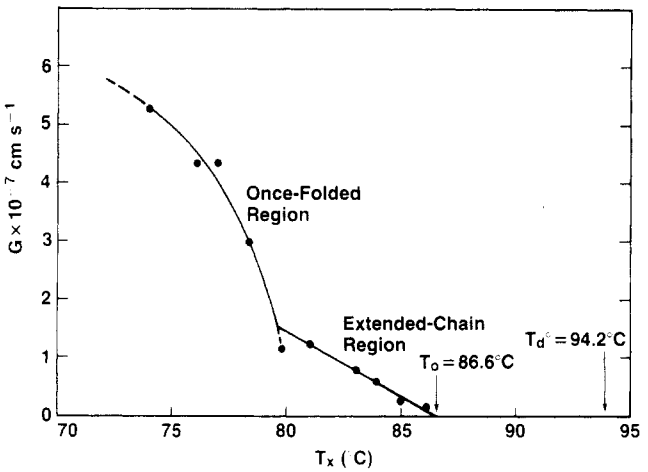

Figure 4. Growth rate of isolated extended-chain and once-folded crystals of polyethylene fraction C-207 with $M_w/M_n = 1.07$ from 0.05% xylene solution as a function of isothermal crystallization temperature. Slope in extended-chain region is $K \cong 2 \times 10^{-8}$ cm s^{-1} deg^{-1} (after Leung and Manley[7]). The solid line through the points in the extended-chain region is closely approximated by eq 53 with $\sigma(1-\gamma) = 10.52$ erg cm^{-2}. For $\gamma = 0.1$, this gives $\sigma = 11.67$ erg cm^{-2}. Note the different shapes of the growth rate curves in the extended-chain and chain-folded regions.

at very low $T_0 - T$ where the exponential in $1 - \exp[-W(T_0 - T)$ can be expanded and where ψ does not affect $G(T)$. At the large $T_0 - T$ involved in C-207 this is not exact, and large deviations in a downward direction from the linear growth law appear in G_B' for $\psi = 0$ at moderate and large $T_0 - T$. Nevertheless, we shall proceed to estimate $\sigma(1-\gamma)$ with the simpler expressions and then show that the resulting $\sigma(1-\gamma)$ is very little in error by using the exact expression as given in eq 33c, demonstrating in turn that the simpler procedure is actually quite satisfactory for obtaining a preliminary estimate of $\sigma(1-\gamma)$.

Rate data are given by Leung and Manley for various concentrations of polymer. All the runs exhibited the linear law in the extended-chain region of the type shown in Figure 4, and all extrapolated to the same T_0. The growth rate at various concentrations (c = weight percent of polymer) at a given temperature below T_0 is quite accurately represented[7,19] as varying as $c^{0.4}$. From their data, including those shown in Figure 4, we find

$$G \text{ (cm s}^{-1}) = (T_0 - T)(6.8 \times 10^{-8} c^{0.4}) \quad (50a)$$

i.e., as $c \to 1$

$$K_{exptl} \text{ (cm s}^{-1} \text{ deg}^{-1}) \cong 6.8 \times 10^{-8} \quad (50b)$$

This value of K_{exptl} will be used in the calculations to follow in order to minimize the effect of varying concentration. We shall now analyze this K using model B for each regime to obtain an estimate of $\sigma(1-\gamma)$ by way of eq 32b and 33b. In calculating σ from eq 32b, we use the values of a_0, b_0, and Δh_f given previously for C-94, and let $\bar{l} = l_x = 207 \times 1.27 \times 10^{-8} = 2.629 \times 10^{-6}$ cm, $T_m \to T_d^\circ = 367.4$ K, and the mean crystallization temperature $T = \bar{T} = 356$ K. For the regime I calculations, n_s has mostly been set at 2.2×10^3, corresponding to $L = 1$ μm. The same range of C_0 values as was used for C-94 is employed here for the regime II calculations. We have used eq 10a for β_g, and set $Q^* = 2000$ cal mol^{-1} as an estimate of the activation energy for transport in solution. (We do not use the reptation model in dilute solution.) The value of σ_1' is allowed to vary from zero to 5 erg cm^{-2}. The calculations were carried out in the same manner as for C-94 and with K_{exptl} lead to the expressions where σ is in erg cm^{-2}

$$\sigma(1-\gamma) = 5.87 + 0.225 \ln (C_0 n_s) - 1.73 \times 10^{-2}\sigma_1' \quad \text{(regime I)} \quad (51)$$

$$\sigma(1-\gamma) = 11.89 + 0.225 \ln C_0 - 3.46 \times 10^{-2}\sigma_1' \quad \text{(regime II)} \quad (52)$$

As is clear from eq 51 and 52, one can only find $\sigma(1-\gamma)$ directly from growth rate data on fractions. The values of $\sigma(1-\gamma)$ derived from eq 51 and 52 are given in Table III. Application of the Lauritzen Z test using eq 42c with $W = a_0 b_0 l_x (\Delta h_f)/k\bar{T}T_d^\circ = 0.771$ and any allowable value of ψ^* and γ gives $Z \ll 0.1$ for the regime I $\sigma(1-\gamma)$ data, and $Z \ll 1$ for the regime II data. The result is therefore decisive: only regime I can possibly be correct for C-207 in the extended-chain region. Accordingly, we shall deal henceforward only with regime I. Note that $\sigma(1-\gamma)$ is but

little affected by a change in σ_1', the end surface free energy of the first (nucleating) stem. Observe also that $\sigma(1-\gamma)$ does not vary strongly even with very large changes in N_0. The estimation of σ from $\sigma(1-\gamma)$ is deferred until after the exact calculations of $\sigma(1-\gamma)$ and ψ^* have been given.

An analysis of the C-207 data was carried out by using the more exact expression for regime I, eq 33c, which is applicable at all $T_0 - T$ in the extended-chain region. The calculations outlined below were carried out with eq 33c for $C_0 = 10^4$, $n_s = 2.2 \times 10^3$, i.e., $N_0 = 2.2 \times 10^7$, $Q^* = 2000$ cal mol^{-1}, $\sigma_1' = 0$, $\sigma' = 76$ erg cm^{-2}, and the values of a_0, b_0, l_x, T_0, and Δh_f given earlier. These fix the preexponential factor $C_0 n_s b_0 (kT/h)$ at 6.768×10^{12} cm s^{-1} and W at 0.771 deg^{-1} giving, with the empirical concentration factor included

$$G_B' \text{ (cm s}^{-1}) = c^{0.4}(6.768 \times 10^{12})\{[1 - e^{-0.771(T_0-T)}]e^{0.771\psi^*(T_0-T)}e^{2081.74\psi^*/T}\}e^{-1006.5/T}e^{-1581.21\sigma(1-\gamma)/T} \quad \text{(regime I, all } T_0 - T\text{)} \quad (53)$$

The result of the fit in the extended-chain region (~80–86.6 °C) is

$$\sigma(1-\gamma) = 10.52 \text{ erg cm}^{-2} \quad (54)$$

$$\psi^* = 0.529 \quad (55)$$

The value of $\sigma(1-\gamma)$ given above is very narrowly bounded. Moreover, the value of $\sigma(1-\gamma)$ found by the more exact procedure is fairly close to the result $\sigma(1-\gamma) = 9.67$ erg cm^{-2} given in Table III for the regime I case where $C_0 = 10^4$, $N_0 = 2.2 \times 10^7$, and $\sigma_1' = 0$, so that it is clear that the simpler procedure represented by eq 51 is satisfactory as a first approximation with regard to estimating $\sigma(1-\gamma)$ from the growth rate data. The ψ^* given above tends to be determined by the data at the larger $T_0 - T$; the value of ψ^* is irrelevant to the fit at very low $T_0 - T$. There is some indication that ψ^* falls somewhat with decreasing temperature.

A value of $\sigma(1-\gamma)$ as calculated for $C_0 = 10^2$, $N_0 = 2.2 \times 10^5$, $\sigma_1' = 0$, $\sigma' = 76$ erg cm^{-2}, and $Q^* = 2000$ cal mol^{-1} by the exact procedure is given in parentheses in Table III, together with the corresponding ψ^*. For the most probable values of C_0, which range from ~10^2 to ~10^4, the "best" values of $\sigma(1-\gamma)$ run from ~9.4 to ~10.5 erg cm^{-2}.

If eq 53–55 are used, all the growth rate data of Leung and Manley at various concentrations in the extended-chain region are reproduced, even at large $T_0 - T$, including those shown for $c = 0.05\%$ in Figure 4. A similar match of the data is obtained if the $\sigma(1-\gamma)$ and ψ^* values relevant to $N_0 = 2.2 \times 10^5$ shown in Table III in parentheses are employed in eq 53, the preexponential factor now being 6.768×10^{10}. Thus, the $G \propto T_0 - T$ growth law is explained in detail over the range where extended-chain growth is observed. The empirical concentration dependence factor $c^{0.4}$ calls for a fundamental explanation, but we shall not address this problem here except to mention a possible physical origin for it.[19]

It is necessary to have an estimate of γ in order to calculate σ from $\sigma(1-\gamma)$. While the existence of a γ greater than zero for a fraction does not pose a conceptual problem—it is easy to understand that a chain somewhat shorter than the average that has a low end surface free energy σ_1' must nucleate the substrate—it is difficult to obtain a solid estimate of this quantity. However, one knows from the $T_d°$ studies of Leung and Manley that molecules shorter than ~C-100 have a dissolution temperature below the T_0 of 86.6 °C found for C-207. This suggests an absolute upper bound for γ of ~$^1/_2$. But a molecule as short as C-100 would have a much reduced driving force Δf for crystallization (including primary nucleation) at $T_0 = 86.6$ °C, and it would therefore appear that a γ in the range of perhaps 0.1–0.2 is more reasonable. To be conservative, we shall choose $\gamma \sim 0.1$ and quote σ as being about 11 erg cm^{-2} based on the calculations for $\gamma = 0.1$ in Table III that are derived from the "exact" $\sigma(1-\gamma)$ values. We would estimate the lower bound of σ as ~10.5 erg cm^{-2} as for the case $C_0 = 10^2$ and $\gamma = 0.1$; it is doubtful if σ is larger than ~15 erg cm^{-2}, corresponding to $C_0 = 10^4$, $\gamma = 0.3$ (Table III). In no case do we see any compelling evidence suggesting that σ for C-207 is impossibly low for an n-hydrocarbon. Through eq 33d the choice $\gamma = 0.1$ leads to ψ values of ~0.55–~0.60. It is interesting to note in this connection that a value of $\psi = 0.38$ was found for chain-folded i-polystyrene by fitting the lamellar thickness l_g^* as a function of crystallization temperature.[1] Here also the data at the larger undercoolings played the main role in determining ψ.

It is concluded that the rough end σ'-type surface characteristic of a polydisperse fraction in the extended-chain form leads through a large surface free energy σ' to a T_0 far below $T_d°$ in C-207; the low T_0 appears in full because C-207 grows from solution as an isolated crystal. The $G \propto T_0 - T$ extended-chain growth law is explained in detail, even at large $T_0 - T$. The growth in the extended-chain region is nucleation controlled and conforms to regime I kinetics. It is concluded further that σ is roughly 11 erg cm^{-2}. The principal uncertainty in this value arises from effects associated with the polydispersity of the sample. It appears reasonable in a fraction crystallizing in the extended-chain mode that the primary nucleation act will involve a stem somewhat shorter than the average value $\bar{l}$; this results in a "σ" value that is noticeably lower than the true lateral surface free energy. It is evident that when T_0 is found to be well below T_m or $T_d°$ for an extended-chain system, the "σ" that is found from kinetics is actually $\sigma(1-\gamma)$.

We mention here the work of Simon, Grassi, and Boistelle[20] on the growth of C-32 from petroleum ether solutions. We have not attempted to employ the theory of growth given in their paper to C-207, since it applies only to crystallization where a single large surface patch is assumed to form on the face of many contiguous lamellae forming a large continuous growth face (two-dimensional nucleus), whereas in the case of C-207 growth is definitely confined to the edge of a single lamella. This corresponds to the case that we have explicitly treated. The type of surface nucleus proposed by Simon and co-workers does not lead to a $G \propto T_0 - T$ law near the melting point.

VI. Discussion

The linear growth rate of the form $G = K(T_0 - T)$ predicted for extended-chain crystallization is confirmed for C-94 at low values of $T_0 - T$. A linear law is found in C-207 over a wide range of $T_0 - T$, but at large $T_0 - T$ this proves to be caused partly by the fact that $\psi > 0$. The intervention of ψ is unimportant at low $T_0 - T$ and plays no role in the C-94 analysis.

Observe that the $G_{\text{extended-chain}} \propto T_0 - T$ law is very different from that governing chain-folded crystallization, which is of the form[1] $G_{\text{fold}} \propto \exp[-K_g/T(\Delta T)]$. As T_m or $T_d°$ is approached, G_{fold} falls off very rapidly in an "accelerated" exponential manner, while as T_0 is approached $G_{\text{extended-chain}}$ descends in a linear fashion. The inadvertent application of the G_{fold} expression to extended-chain growth would lead to a very low "K_g" value, and the resultant low "$\sigma\sigma_e$" would have no physical meaning.

We recall here a point made earlier, namely, that the $G \propto \Delta T$ law appropriate to surface nucleation-controlled

growth in extended-chain systems at low ΔT was first demonstrated theoretically for regime I by Lauritzen, Passaglia, and DiMarzio.[12] In their treatment, as in ours, the prediction of the $G \propto \Delta T$ law is inevitable in regime I at very low undercoolings so long as the substrate length L is approximately constant. Here we have shown on theoretical grounds that this result applies as well to regime II, there being no restriction on the behavior of L in this case. In both regimes, this simple growth law arises at low $T_0 - T$ directly from an appropriate consideration of the flux (A–B) associated with the substrate completion process. As we have shown earlier, the persistence of the $G \propto T_0 - T$ law at larger $T_0 - T$ is a result of more complex causes (see eq 33 and 53). Here it is seen that the approximate linearity involves a competition between a factor containing ψ that augments the nucleation and substrate completion rates with decreasing temperature (i.e., increasing $T_0 - T$), and factors such as $\exp[-2b_0\sigma(1-\gamma)l_x/kT]$ that, with fixed l_x, decrease the nucleation rate with decreasing temperature. The balance between the two effects is a rather sensitive one, and deviations from a linear dependence of G on $T_0 - T$ must be anticipated at sufficiently large $T_0 - T$. In the case of C-207, no significant deviation from linearity was noticed in the ~7 °C interval where extended-chain growth rates were observed (Figure 4). In this case, chain folding intervened before any large deviation occurred. The onset of "once-folding" in such circumstances is of course not surprising (see later).

The discussion to follow of the behavior of σ as a function of morphology and chain length will be more complete if we bring homogeneous nucleation data on short n-paraffins into the picture.

Turnbull and Spaepen[21] have analyzed homogeneous nucleation data on n-paraffins C-15–C-32 under the assumption $\sigma' = \sigma$ for a three-dimensional nucleus. From the "scaled crystal-melt interfacial tension" value of $\bar{\alpha}_1 = 0.15$ which they derived from these data one finds the constant value $\sigma = 12.1$ erg cm^{-2} for C-15–C-32 (see later for definition of $\bar{\alpha}_1$). A strong upswing in $\bar{\alpha}_1$ or σ calculated in this manner occurs below C-15, which was explained by these authors in terms of the effect of short trans sequences in the liquid state using the so-called "negentropic" model. We note, however, that if σ' in a pure compound is considerably smaller than σ, the three-dimensional nucleus model is modified. The reason is that the three-dimensional nucleus model has the critical length $l^* = 4\sigma'/(\Delta f)$, and if σ' is small, this may be very close to l_x. Oliver and Calvert[22] have shown using a cylindrical monolayer homogeneous nucleus, for which the critical free energy of formation is $\Delta\phi^* = \pi l_x\sigma^2/(\Delta f)$ for $\sigma \gg \sigma'$, that homogeneous nucleation data in the range C-16–C-28 give $\sigma = 12.7 \pm 1.6$ erg cm^{-2}. Below C-16, the values of σ increase noticeably; there is a hint of a remnant of this effect above C-16. The explanation for this upswing is presumably the same as that suggested by Turnbull and Spaepen. Whichever model of the extended-chain homogeneous nucleus is correct, the homogeneous nucleation data on the n-paraffins ~C-15 and longer lead to σ values that are quite similar to those we had found earlier for chain-folded crystallization in polyethylene, and the values found here for C-94 and C-207 (Table IV).

The near coincidence of σ as found in the homogeneous nucleation studies on the pure n-paraffins ~C-15 and longer with that for pure C-94 as determined from the growth rate has important consequences for the theory of nucleation-controlled growth in extended-chain systems. The σ associated with the large homogeneous nucleus, whether the nucleus be three-dimensional or monolayer in character, clearly refers to a lateral surface consisting of full stems of length l_x, and *not* partially attached stems. Then if essentially the same σ is found in growth rate studies on a pure extended-chain system as is found for homogeneous nucleation, it is reasonable to conclude that the rate-determining step in surface nucleation in the pure extended-chain compound also refers to the energetics of the deposition of a full stem of length l_x, or a close approximation to it. Thus, we do not at this juncture see a need to postulate a surface nucleation model for a pure compound where the surface nucleus builds up piecemeal by successive addition of parts of stems of different molecules.

The foregoing merits further comment. A key feature of a "partial stem" surface nucleus model is that during its formation the unattached portions of each molecule are persistent random-coil type cilia to which one must assign a substantial end surface free energy. The view that extensive ciliation leads to high end surface free energies is strongly supported by the behavior of extended-chain crystallization in systems where ciliated end surfaces are known to exist by virtue of the presence of a distribution of chain lengths. If ciliation cannot be avoided, as in the overall end surface of an impure compound or polydisperse fraction, a high effective end surface free energy σ' that retards crystallization by preventing substrate completion in an isolated lamella is incurred forthwith. The large σ' of ca. 76 erg cm^{-2} resulting from the rough (i.e., partially ciliated) end surface in the fraction C-207 that prevents crystallization altogether until an undercooling of 7.6 °C is attained fully illustrates this point (see Figure 4). This shows that persistent adjacent cilia on the σ'-type surface lead to substantial end surface free energies and clearly implies that a "ciliated" surface nucleus made up of many partially attached stems of different molecules could readily find itself in serious energetic difficulties.

From the above, it is concluded that it is a reasonable approximation to assume, as has been done in this paper, that the initiating process in surface nucleation in a pure extended-chain compound relates to the energetics associated with the deposition of a "first" stem of length l_x. It would appear that the large end surface free energy associated with the considerable number of cilia inherent in the successive partial stem addition model mutes its importance in extended-chain crystallization. In a fraction, the somewhat shorter-than-average first stem can attach to the substrate without any excessive end surface free energy resulting from pendant cilia.

The results of the value of σ determined in various ways is summarized in Table IV. Chain lengths from ~C-15 to moderate molecular weight polyethylene corresponding to ~C-8140 are covered, and both the extended-chain and the chain-folded morphology are included. We see no general evidence that σ in the n-hydrocarbon system varies markedly with chain length or morphology or takes on any inexplicably low values. Evidently σ is a genuine physical quantity of broad applicability and is thus not a parameter that appears in an unsupported manner in the theory of polymer crystallization with chain folding. On a broader basis, the precepts underlying nucleation theory appear to be tenable for growth in the extended-chain mode of both pure compounds and fractions, for chain-folded lamellar growth in polyethylene, and for homogeneous nucleation in the n-paraffins ~C-15 and longer.

Conclusions quite different from the above concerning the properties of σ in the extended-chain region were reached by Point and Kovacs for poly(ethylene oxide) fractions.[6] Values of σ that were very low (in one bound

Table IV
Estimates of the Lateral Surface Free Energy σ for *n*-Hydrocarbon Systems

	compd and morphology	data source	method	σ^a, erg cm^{-2}	remarks
1	highly purified C-94 crystallized from melt (extended-chain morphology)	this work	*growth rate*: σ from K in $G_{A,C} = K(T_0 - T)$	13.8 ± 2.1	mixed regimes I and II
2	polyethylene fraction $M_n = 2900$ corresponding to C-207 crystallized from dilute xylene solution (extended-chain morphology)	Leung and Manley[7]	*growth rate*: σ from K in $G_B' = K(T_0 - T)$	about 11	regime I; principal uncertainty results from polydispersity of sample (see text)
3	polyethylene fractions $M_w = 2.36 \times 10^4$ to 1.14×10^5 crystallized from melt, C-1690 to C-8140 (chain-folded morphology)	Hoffman[2] for $\sigma\sigma_e$ from $G(T)$; Huseby and Bair[23] for σ_e (see also ref 1)	*growth* rate: $\sigma\sigma_e = 1065$ erg^2 cm^{-4} from K_g in $G(T) \propto \exp[-K_g/T(\Delta T)]$ for PE fractions; σ_e = 90 erg cm^{-2} from T_m' vs. $1/l$ plot; same value of $\sigma\sigma_e$ valid in both regimes I and II; σ calculated as $\sigma\sigma_e/\sigma_e$.	12.0 ± 1.2[b] (values from 11 to 14 quoted in the literature[1,2])	same σ valid in both regime I and II; regime transition observed experimentally[2]
4	pure *n*-paraffins C-15–C-32 (extended-chain morphology)	Turnbull and Spaepen;[21] Oliver and Calvert[22]	*homogeneous nucleation rates*	12.1 for three-dimensional nucleus with $\sigma = \sigma'$ (C-15–C-32);[21] 12.7 ± 1.2 for cylindrical monolayer nucleus for $\sigma' \ll \sigma$ (C-16–C-28)[22]	

[a] The average of the central values of σ for all methods listed in this column other than item 2 (C-207) is 12.7 ± 1.2 erg cm^{-2}. [b] The error of ±1.2 erg cm^{-2} quoted here is based on the estimated uncertainty in $T_m°$ for polyethylene which is given as[8] $T_m° = 145.5 \pm 1$ °C.

as low as ~0.3 erg cm^{-2}) and dependent on chain length were proposed. (No important anomalies concerning σ were noted by these authors in the high molecular weight region where chain folding occurred; here the value of σ from growth kinetics appears to be close to the value of ~11 erg cm^{-2} that one would calculate from eq 56 or 57, to be given shortly.) The conclusion of Point and Kovacs concerning the presence of irreducible and fundamental flaws in nucleation theory based on their work on extended-chain poly(ethylene oxide) fractions may have arisen from the presence of a mode of growth very different from that which occurs in the corresponding *n*-hydrocarbons. We are unable to calculate $\sigma(1 - \gamma)$ from their published data by the slope method outlined in the present paper, since initial slopes beginning near T_0 are not reported for their fractions. We note that no account was taken of the possibility that polydispersity may have affected their results.

From the new determination of σ given in this work for C-94, together with those listed under items 3 and 4 in Table IV, we find the mean value 12.7 ± 1.2 erg cm^{-2}. This gives the following value of the useful semiempirical parameter α:[1]

$$\alpha \equiv \sigma/\Delta h_f(a_0 b_0)^{1/2} = 0.104 \pm 0.010 \qquad (56)$$

(This α should not be confused with that in the empirical concentration-dependence factor c^α.) The corresponding value of $\bar{\alpha}_1$, the "scaled crystal-melt interfacial tension" as given by Turnbull and Spaepen,[21] has the definition and value

$$\bar{\alpha}_1 \equiv \sigma/\Delta h_f(a_0 b_0 l_u)^{1/3} = 0.158 \pm 0.016 \qquad (57)$$

The quantities given above differ but little from the $\alpha \cong 0.1$ used by us in many applications,[1] and the value $\bar{\alpha}_1 \cong 0.15$ given by Turnbull and Spaepen for *n*-paraffins C-15–C-32.

The α and $\bar{\alpha}_1$ values noted above are smaller by a factor of about 2–3 than those for nonchain molecular crystals of otherwise similar chemical constitution. The negentropic model employed by Turnbull and Spaepen represents one interesting approach to this question. While $\alpha \cong 0.1$ evidently applies to many polymers for the purpose[1] of estimating σ, the negentropic model would allow deviations in some cases with the result that this value should probably not be regarded as necessarily applicable to all chain systems. The origin of the fold surface free energy σ_e is already well understood, the main contribution being the work q required to bend the chain back on itself.[1]

The treatment given here highlights some intriguing questions that relate to nucleation-controlled crystal growth. Among these is the origin of the substrate length $L = n_s a_0$. The importance of this quantity in nucleation-controlled growth is in no way diminished by the fact that there was no need to know its exact value in the present study. It is clear that L is a real quantity. This is shown

by the undoubted existence[1,2] of regime I → regime II transitions in chain-folded systems, which cannot be explained without reference to a substrate length L. When such regime transitions are found, as in the case of polyethylene fractions,[2] the value of L can be estimated as about 0.8 μm, at least within a factor of 2 or so. The question of the true origin of L deserves further experimental and theoretical effort. For the time being, we regard it as a "persistence length" between events such as defects that terminate strip completion.

Regime II growth permits local surface roughness on the growth front, so "perfect" facets are not expected. C-94 grew in a "mixed" regime I and II mode, so such an effect was possible in this case. The somewhat rounded edges that were sometimes seen behind the (apparently) faceted growth tips may have some connection with this "mixed" regime effect. The origin of the curved edges merits attention. Conversely, extended-chain C-207 was strictly regime I, which is consistent with the well-defined 110 facets that were observed.[7]

Another and related challenge concerns C_0, which governs the absolute growth rate of both extended-chain and chain-fold crystallization in regime II. The accuracy with which C_0 is known from experiments on polyethylene fractions[2] is quite sufficient to permit the determination of σ or $\sigma(1 - \gamma)$ within rather narrow limits as we have shown. Nevertheless, the theory of this preexponential factor merits attention.

An issue of theoretical interest concerns the factor ψ that states the balance between the rates of the forward and backward reactions in the fundamental rate constants A_0, B_1, A, and B.[11] Here we have found it experimentally to be about 0.55 to 0.60 for C-207. (We note that the ψ associated with A_0 and B_1 is dominant in determining $G(T)$ and l_g^* at large undercoolings.) It is a mistake to regard ψ simply as a parameter that allows theory to match data—there *is* actually a balance between the rates of the forward and backward reactions, and the theoretical problem of its origin ought to be addressed. Though frequently ignored, a factor of the type of ψ is present though veiled in many physical systems where the rates of forward and backward reactions are considered on a microscopic scale. It is fortunate that nucleation experiments bring this factor to light in a manner such that it cannot be disregarded.

Despite the consistency of the value of σ that has emerged, the present study by no means forecloses the need for further experimental tests of nucleation-controlled growth in the extended-chain region in the n-paraffins. One approach would be to measure K_{exptl} for a pure n-paraffin such a C-100 crystallizing from the melt. Then σ could be determined from the ratio $K_{\text{C-94}}/K_{\text{C-100}}$ without reference to estimates of L, C_0, or Q^*. Corresponding work on melt-crystallized fractions would be of interest, but would only be useful if T_0 was known for each member. Even then, one would only obtain $\sigma(1 - \gamma)$ rather than σ, as we have shown here. Thus, from the standpoint of checking the tenets of nucleation theory as applied to extended-chain crystallization, we would assign the higher priority to work on pure compounds. It would however be of interest to carry out melt-crystallization studies on C-207 and similar fractions to determine $\sigma(1 - \gamma)$ and T_0 for purposes of comparison with the results derived here from data on solution growth rates. For the purposes of dealing more precisely with fractions, it would be most useful to have a theoretical treatment of γ.

The fact that coherent nucleation, at least in broad aspect, appears successfully to predict the major features of the growth rate in chain systems invites comment. As pointed out by Keith and Passaglia,[24] it is on energetic grounds difficult to justify the formation of a screw dislocation on the σ-type surface, i.e., one with its Burger's vector parallel to the G direction shown in Figure 1. This paves the way for coherent surface nucleation to act as the dominant mechanism for growth of the lateral faces, i.e., in the direction perpendicular to the chain axes, in chain systems. Screw dislocations are of course known in extended-chain systems, but they are not associated with the lateral growth faces. As we have shown here, the observable growth rate in extended-chain systems shows considerable evidence of being nucleation controlled.

It seems worthwhile to comment on the overall status of our present knowledge concerning the onset of chain folding with increasing molecular weight and undercooling in the n-hydrocarbon system. The current study provides an improved understanding of the growth rate of both pure extended-chain n-hydrocarbons and fractions in the region ~C-100–~200, where the growth law is of the form $G \propto T_0 - T$. Further, nucleation theory as combined with the concepts of reptation and regime theory[2,25], together with a knowledge of the topological constraints on nonadjacent reentry noted in the "gambler's ruin" and related calculations,[26-28] leads to a basic perception of the origin of chain folding and the rate of crystallization with chain folding in the high molecular weight n-hydrocarbons, such as the polyethylene fractions C-1690–C-8140 referred to in Table IV. Specifically, the growth rate in this molecular weight range is understood within reasonable limits as a function of temperature, regime, and molecular weight.[25] The initial lamellar thickness is also predicted.[1,25] The growth law in the chain-folded case is of the form[1] $G_{\text{fold}} \propto \exp[-K_g/T(\Delta T)]$ because the long molecules tend to fold back on themselves during crystallization partly because of topological constraints and in effect choose their own nucleus length $l_g^* = 2\sigma_e/(\Delta f) + \delta$. (Some of these points are briefly summarized in a recent review.[29]) The shape of the G_{fold} vs. T curve is in general rather like that shown for the "once-folded" case in Figure 4; i.e., it descends very rapidly with increasing T_x and thus differs in kind from the $G_{\text{extended-chain}} \propto T_0 - T$ case. In the case of extended-chain crystallization, the nucleus length is fixed at the molecular length l_x, which is basically what leads to the different growth rate law for such systems.

The details of the growth process in the region of intermediate chain length, where the chains are once and twice folded, are less well understood, though there is evidence in the work of Leung and Manley[7] that the chain-fold theory is tenable at least in a general way even down to molecular weights where the chains are only three times folded. An example of the nature of the onset of the once-folded region is shown in Figure 4. Elucidation of the full range of behavior in the once- and twice-folded region stands as both an experimental and interpretive challenge.

We close by remarking that there is no difficulty in perceiving in the context of what has been shown here for extended-chain crystallization why in a general sense chain folding prevails at high molecular weights and high undercoolings. At a fixed undercooling, extended-chain growth will become exceedingly slow at some chain length l_x because $i_{\text{extended-chain}} \propto \exp(-2b_0\sigma l_x/kT)$ so that $G_{\text{extended-chain}} \propto \exp(-2b_0\sigma l_x/kT)$. Then if the chain is long and flexible enough to fold, it will choose its own characteristic stem length $l_g^* \cong 2\sigma_e/(\Delta f) + \delta = 2\sigma_e T_m/(\Delta h_f)(\Delta T) + \delta$ where $l_g^* < l_x$, pay the price of the work of chain folding $q = 2a_0b_0\sigma_e$ in the substrate completion process,

and grow according to $G_{fold} \propto \exp[-2b_0\sigma l_g^*/kT] \propto \exp[-K_g/T(\Delta T)]$ where K_g now contains the product $\sigma\sigma_e$. At sufficiently large l_x and ΔT, it is thus certain that $G_{fold} > G_{extended\text{-}chain}$. In the case of higher molecular weights where $l_g^* \ll l_x$, the folding process retains its dominance because of topological constraints; it has been shown unambiguously that for vertical stems close to two out of three events in the substrate completion process must involve adjacent or very near adjacent reentry returns to prevent a density paradox at the lamellar surface.[26-28] This requirement is not mitigated by the presence of a semiordered interfacial layer,[27] though some relief can be achieved by tilting.[2,26,28] Thus, the onset of chain folding with increasing chain length and undercooling is at first a matter of relative rates and chain flexibility, and its prevalence at high molecular weights is further assured by topological considerations.

VII. Summary and Conclusions

Our principal findings and conclusions are as follows:

(1) One important overall conclusion, valid on theoretical and experimental grounds, is that though nucleation-controlled growth is involved in both instances, the growth rate law for extended chains is entirely different from that for chain-folded growth. The difference arises from the fact that in chain-folded growth, the long molecules choose their own nucleus stem length l_g^* as a variable that befits the prevailing undercooling, while in the extended-chain case with shorter molecules the stem length of the nucleus is fixed at the molecular length l_x for a pure compound and $l_x(1-\gamma)$ for a fraction. This result has important consequences, and specifics are given below with emphasis on extended chains.

(2) A simple treatment of the growth rate in a monodisperse extended-chain system based on surface nucleation theory with fixed nucleus length l_x leads to a growth law of the form $G = K(T_0 - T)$ at very low undercoolings for both regimes I and II. Here T_0 is a crystallization onset temperature extremely close to T_m or $T_d°$. (A law of this general form was first given for regime I by Lauritzen, Passaglia, and Dimarzio.[12]) This $G_{extended\text{-}chain} \propto T_0 - T$ law is verified near the melting point for highly purified C-94, and the K value leads to a lateral surface free energy of $\sigma = 13.8 \pm 2.1$ erg cm^{-2}. This is a new type of determination of σ. Application of the Lauritzen Z test shows that growth in C-94 is mixed regime I and II.

(3) The theory was adapted to polydisperse systems with extended-chain growth, including that in dilute solution. This too yields $G = K(T_0 - T)$ at low $T_0 - T$ for both regimes I and II, but with T_0 now being well below T_m or $T_d°$. A key feature is that the primary surface nucleation act is the attachment of a stem of length $\bar{l}(1-\gamma)$ where $\bar{l}$ is the mean length of the molecules in the fraction; this leads the "σ" that is determined from growth rate data on fractions to actually be $\sigma(1-\gamma)$, i.e., lower than the true σ. The theory is extended by the introduction of ψ to include large $T_0 - T$. Application to a polyethylene fraction corresponding to C-207 crystallizing from solution verifies the $G = K(T_0 - T)$ law over a wide range of $T_0 - T$ (regime I) and yields a σ of roughly 11 erg cm^{-2}. The analysis of C-207 highlights the difficulties encountered in obtaining σ from growth rate data on fractions—the problem is largely that of estimating γ. The growth law for chain-folded systems, where the nucleus length is a variable that depends on the undercooling, is of the entirely different form $G_{fold} \propto \exp[-K_g/T(\Delta T)]$. (See Figure 4).

(4) Another overall conclusion relates to the magnitude and behavior of σ in various applications of nucleation theory. On the basis of the σ for C-94 and C-207, cited above, and the fact that σ from studies on chain-folded polyethylene growth kinetics is similar to these, it is concluded that the quantity σ is not a freely adjustable parameter, but instead a physically meaningful quantity that plays substantially the same energetic role in extended-chain crystallization in short molecules as it does in chain-folded crystallization in very long ones. This is supported further by the fact that homogeneous nucleation studies on short chains ~C-15 and longer give σ values much like those just noted. Thus, one finds a consistent picture regarding σ for extended-chain growth in pure chain compounds and fractions, chain-folded growth in polymers, and homogeneous nucleation of short chains in the n-hydrocarbon system ~C-15 and longer (Table IV).

(5) Considering all the different methods used to determine σ, the "best" value is 12.7 ± 1.2 erg cm^{-2} for the n-hydrocarbons (Table IV). This gives $\alpha = 0.104 \pm 0.010$ and $\tilde{\alpha}_1 = 0.158 \pm 0.016$.

(6) As predicted, the value of the exposed end surface free energy σ' is quite large for an impure extended-chain compound or polydisperse fraction, this phenomenon being induced by the inherent roughness (ciliation) of the end surface. It is a large σ' of this type that causes T_0 for an individual lamella to be well below $T_d°$ in the fraction C-207. It is suggested that σ' for the smooth (methyl group) end surface in a pure n-paraffin is either comparable to or smaller than σ.

(7) It is concluded that one commonly used postulate of surface nucleation theory, namely, that the free energy cost of the first step in such nucleation depends directly on the length of the first stem, appears to be plausible in the n-hydrocarbon system. In the case of a fraction, a stem that is somewhat shorter than the mean will nucleate the substrate.

(8) The impact of the present findings concerning the nature of extended-chain crystallization on the question of the onset of chain folding with increasing molecular weight and undercooling is discussed.

(9) Some important experimental and theoretical challenges remaining in the area of nucleation-controlled growth in chain systems are noted and discussed.

Acknowledgment. The study of C-94 was suggested many years ago by the late Dr. J. I. Lauritzen, Jr., for the express purpose of gaining information on σ, and the experimental work was carried out at the National Bureau of Standards by Drs. G. S. Ross and Lois Frolen Ross shortly thereafter. The author recalls many insightful conversations with Dr. Lauritzen concerning the work, which are herewith acknowledged. Special thanks are also due Drs. G. S. Ross and L. F. Ross for carrying out the careful measurements on C-94, and for recent discussions concerning them. The author also wishes to thank Drs. E. Passaglia, F. Khoury, E. A. DiMarzio, and C. M. Guttman of NBS for important and helpful discussions. Further, we thank Dr. John Crissman of NBS for supplying the zone-refined sample of C-94, and Professor R. St. John Manley of McGill University for providing the growth rate data on C-207 prior to publication, and for highly useful discussions. A portion of the analysis was carried out with the support of grant DMR 84-03358 of the Polymers Program, Division of Materials Research, of the National Science Foundation.

Registry No. polyethylene (homopolymer), 9002-88-4; tetrananacontane, 1574-32-9.

References and Notes

(1) Hoffman, J. D.; Davis, G. T.; Lauritzen, J. I., Jr. In "Treatise on Solid State Chemistry"; Hannay, N. B., Ed.; Plenum Press: New York, 1976; Vol. 3, Chapter 7, pp 497–614.
(2) Hoffman, J. D. *Polymer* **1982**, *23*, 656.

(3) Mandelkern, L. *Discuss. Faraday Soc.* **1979**, *No. 68*. See discussion remarks on pp 414-5.
(4) Wunderlich, B. *Discuss. Faraday Soc.* **1979**, *No. 68*. See discussion remarks on pp 417-9.
(5) The T_m' vs. $1/l$ plot[1] gives an estimate of both $T_m°$ and σ_e. The interplay between the $\sigma\sigma_e$ from the kinetic data using this $T_m°$, and the σ_e from the same T_m' vs. $1/l$ plot, is such that σ always falls between about 11 and 14 erg cm^{-2} for $T_m°$ values running from 141.5 to 146.5 °C because of compensating effects in the analysis. All the disputed values of $T_m°$ for polyethylene are within these limits.[3,4]
(6) Point, J. J.; Kovacs, A. J. *Macromolecules* **1980**, *13*, 399.
(7) Leung, W. M.; Manley, R. St. John Post Grad. Lab. Report no. 275; Pulp and Paper Research Institute of Canada, Pointe Claire, Quebec 1983. Three papers based on this work appear immediately preceding this paper in this issue of *Macromolecules*.
(8) Flory, P. J.; Vrij, A. *J. Am. Chem. Soc.* **1963**, *85*, 3548.
(9) Flynn, J. H. *Polymer* **1982**, *23*, 1325.
(10) Lauritzen, J. I., Jr.; Hoffman, J. D. *J. Appl. Phys.* **1972**, *44*, 4340.
(11) In the more general case, the rate constants given in eq 6-9 can be written[1] $A_0 = \beta_g \exp[-2b_0\sigma l_x/kT - 2a_0b_0\sigma'/kT + \psi a_0b_0l_x(\Delta f)/kT]$, $B_1 = \beta_g \exp[-(1-\psi)a_0b_0l_x(\Delta f)/kT]$, $A = \beta_g \exp[-2a_0b_0\sigma'/kT + \psi a_0b_0l_x(\Delta f)/kT]$, and $B = \beta_g \exp[-(1-\psi)a_0b_0l_x(\Delta f)/kT]$ where $0 \le \psi \le 1$. These expressions are consistent with eq 5 and detailed balance for any fixed value of ψ. In the more general case, a different ψ can be assigned to A_0 and B_1 on the one hand, and A and B on the other.[10]
(12) Lauritzen, J. I., Jr.; Passaglia, E.; DiMarzio, E. A. *J. Res. Natl. Bur. Stand., Sect. A* **1967**, *71*, 245.
(13) Lauritzen, J. I., Jr.; DiMarzio, E. A.; Passaglia, E. *J. Chem. Phys.* **1966**, *45*, 4444.
(14) Lauritzen, J. I., Jr. *J. Appl. Phys.* **1973**, *44*, 4353.
(15) Frank, F. C. *J. Cryst. Growth* **1974**, *22*, 233.
(16) Aquilano, D. *J. Cryst. Growth* **1977**, *37*, 215.
(17) Ross, G. S.; Ross, L. F., private communication.
(18) (a) Khoury, F. *J. Appl. Phys.* **1963**, *34*, 73. (b) It is clear from the work of Leung and Manley[7] that prolonged annealing of extended-chain C-207 can lead to the coalescence of the individual platelets producing a (probably somewhat defective) "multilayered" molecular crystal with largely localized chain ends that exhibits an observed dissolution temperature that is far above T_0 and substantially equivalent to $T_d°$. Such crystals must have considerable interpenetration of chain ends from a given interior lamella to the contiguous ones. (See remarks in section II, model B.)
(19) The $c^{0.4}$ concentration dependence of K (and hence the growth rate at a specified $T_0 - T$) may arise from the presence of adsorbed molecules of high surface mobility on the growth surface. This would provide a source of molecules such that the local concentration at the niche is considerably in excess of that in the solution proper, thus giving a K that varied less than the first power of the actual concentration in solution.
(20) Simon, B.; Grassi, A.; Boistelle, R. *J. Cryst. Growth* **1974**, *26*, 77.
(21) Turnbull, D.; Spaepen, F. *J. Polym. Sci., Polym. Symp.* **1978**, *63*, 237.
(22) Oliver, M. J.; Calvert, P. D. *J. Cryst. Growth* **1975**, *30*, 343.
(23) Huseby, T. W.; Bair, H. E. *J. Appl. Phys.* **1968**, *39*, 795.
(24) Keith, H. D.; Passaglia, E. *J. Res. Natl. Bur. Stand., Sect. A* **1964**, *68*, 513.
(25) Hoffman, J. D. *Polymer* **1983**, *24*, 3.
(26) Guttman, C. M.; DiMarzio, E. A.; Hoffman, J. D. *Polymer* **1981**, *22*, 1466.
(27) Mansfield, M. L. *Macromolecules* **1983**, *16*, 914.
(28) Frank, F. C. *Discuss. Faraday Soc.* **1979**, *No. 68*, 7.
(29) Hoffman, J. D. In "Polyethylene 1933-1983", Golden Jubilee Conference, Proceedings of Plastic and Rubber Institute, London, June 1983, pp D3.1 to D3.13.

Rheooptical Response of Rodlike Chains Subject to Transient Shear Flow. 1. Model Calculations on the Effects of Polydispersity

Andrea W. Chow and Gerald G. Fuller*

Department of Chemical Engineering, Stanford University, Stanford, California 94305.
Received July 30, 1984

ABSTRACT: This paper is the first part of a two-part series investigating the flow dynamics of semidilute solutions of rodlike chains. Specifically, the effects of polydispersity are considered. In this paper, numerical solutions of the flow birefringence Δn and the average orientation angle χ for the Doi-Edwards model for monodisperse systems and the Doi-Edwards-Marrucci-Grizzuti model for polydisperse systems are studied. These models, to be tested in part 2 by experimental results on rodlike collagen proteins using the method of two-color flow birefringence, indicate that the rheooptical properties are very sensitive to the high molecular weight components. A polydisperse solution with a small quantity of high molecular weight chains exhibits substantially different behavior than a monodisperse solution, especially under transient flow conditions. In addition, the birefringence overshoot predicted for the rodlike system was found to be much smaller compared to that observed for flexible systems.

Introduction

The flow response to rodlike macromolecules has attracted increased interest recently due to the unique and important properties which can be achieved from incorporating such materials into the processing of a wide range of products. Of particular note is the possibility of producing high-strength fibers and composite materials. Additionally, many biopolymers assume rodlike conformations and the corresponding rheology of these systems is also of interest. In a series of articles, Doi and Edwards[1] have described a molecular model which attempts to describe the dynamics of semidilute solutions of rodlike chains. This model, which is based on the simple rigid-dumbbell model,[2] incorporates a mechanism by which the hindered rotational diffusion of rods in close proximity is accounted for by encapsulating the rods within tubes which restrict their translation normal to the chain axis but leave translation along the axis unaffected. This simple model has been shown to qualitatively predict a variety of observed phenomena including the strong concentration and molecular weight dependencies of many rheological and dynamic properties.[3,4]

In its original form, the Doi-Edwards model of concentrated rodlike chains describes systems of uniform chain length. For dilute solutions in which interparticle interactions are negligible, polydispersity can be treated as a simple extension of the monodisperse case. Any bulk solution property is simply the weighted average of the

0024-9297/85/2218-0786$01.50/0